Facies (2023) 69:6
https://doi.org/10.1007/s10347-023-00664-9

ORIGINAL ARTICLE

Progradation of a shallow carbonate platform developed on a fault-block in the Western Tethys (lower Aptian, Sierra de Bedmar-Jódar, Prebetic of Jaén, Spain)

Rafael Martínez-Rodríguez[1,2] · Luis M. Nieto[1] · José M. Castro[1] · Ginés A. de Gea[1] · Pedro A. Ruiz-Ortiz[1] · José M. Molina[1] · Peter W. Skelton[3]

Received: 13 October 2022 / Accepted: 24 March 2023 / Published online: 10 April 2023

Abstract

The Middle Member of the Llopis Fm in the Sierra de Bedmar-Jódar Unit of the Prebetic Zone of Jaén (southern Spain) was deposited on a shallow-marine platform of the Southern Iberian Continental Margin during the earliest Aptian. Detailed field logging of nine stratigraphic sections and facies mapping have allowed seven lithofacies associations (L1–L6) to be distinguished, one siliciclastic (L1) and five carbonate facies (L2–6). The succession is composed of eight consecutive elemental sequences of lithofacies associations L1–L6. Each elemental sequence is interpreted as representing one episode of shallowing-upwards carbonate deposition in a very shallow platform-lagoon that was bounded shoreward by clastic/ooid bars and passed seaward either to stromatoporoid bioconstructions (bioherms and biostromes) or rudist biostromes. The successive elemental sequences show north-eastward progradational geometries. Three phases of platform development are identified: (1) installation of the shallow platform; (2) development of a lagoon bounded by a stromatoporoid barrier and (3) development of an Urgonian-type platform dominated by rudists. During the early Aptian, the Bedmar-Jódar platform was partially isolated from the rest of the Prebetic platform and showed overall progradation towards the NE, in contrast to the general south-eastward progradational trend of the Prebetic platform. Sedimentation was controlled by rift-generated extensional tectonics that resulted in tilting of the platform block, causing the deviation of progradation from the general trends of the Prebetic Platform. In addition, climatic influence is inferred from the presence of siliciclastic sediments derived from weathering of the hinterland, which restricted the carbonate factory.

Keywords Prebetic · Aptian · Isolated carbonate platform · Progradational sequences · Stromatoporoids · Rudists

Introduction

The break-up of Pangaea during the Mesozoic involved fragmentation of the carbonate platforms that had developed along the Tethyan margins. Rift basins with partially or completely isolated blocks were formed on which shallow-marine carbonate deposition persisted ('fault-block platforms' of Bosence 2005). In the late Early Cretaceous, the largest and most widespread platforms of the entire Mesozoic developed in tropical and subtropical seas from accumulations of shallow-water carbonates rich in rudists, corals, chaetetids and stromatoporoids (Simo et al. 1993; Michalik 1994; Kiessling et al. 2003; Philip et al. 1995; Philip 2003).

The earliest Aptian witnessed a global episode of carbonate platform growth throughout the Tethys/Atlantic and low-palaeolatitude Pacific (seamount) belt (Skelton and Gili 2012). This episode was associated with a major transgression onto the extensive platform margins that were generated by global rifting during the Late Jurassic-Early Cretaceous. Rifting propagated from the Central Atlantic towards the north with linked opening of the Bay of Biscay and counterclockwise rotation of Iberia (e.g. Martín-Chivelet et al. 2019). This earliest Aptian episode of carbonate platform

Peter W. Skelton: Independent Researcher.

✉ Luis M. Nieto
lmnieto@ujaen.es

[1] Dpto. de Geología and CEACTEMA, Universidad Jaén, Campus Universitario, 23071 Jaén, Spain

[2] Dpto. de Paleontología, Estratigrafía y Geodinámica, Universidad Complutense de Madrid, 28040 Madrid, Spain

[3] Milton Keynes, UK

growth was dominated by rudists in low latitudes, which experienced prolific diversification, occupying different platform habitats (Skelton and Gili 2012). The earliest Aptian episode of carbonate platform growth terminated with the onset of OAE1a, which in many cases resulted in the demise of the carbonate platforms (e.g. Weissert et al. 1998; Föllmi 2012; Skelton and Gili 2012; Clavel et al. 2013; Hay et al. 2019; Skelton et al. 2019).

Like other Tethyan margins during the early Aptian (e.g. García-Mondéjar 1990; Masse et al. 1998; Föllmi et al. 2006; Najarro et al. 2011; Amodio et al. 2013), extensive carbonate platforms developed on the shallow (Prebetic) margin of the South Iberian Continental Margin (SICM) (e.g. Castro and Ruiz-Ortiz 1995; Ruiz-Ortiz and Castro 1998; Castro et al. 2008; Martín-Chivelet et al. 2019; Skelton et al. 2019). These platforms were strongly affected by rift tectonics and the development of partially isolated fault-controlled blocks. From a regional perspective, terrigenous sedimentation predominated in the proximal sectors of the Prebetic, whereas an extensive shallow carbonate platform developed in the more marine context of maximum shoreline transgression (e.g. Vilas 2001; Vilas et al. 2004; Martín-Chivelet et al. 2002, 2019; Vera 2004; Castro et al. 2008).

Study of the controls on the development of carbonate successions exerted by eustatic, climatic, and tectonic processes can elucidate their evolutionary trends (Enos and Moore 1983; Eberli and Ginsburg 1989; Schlager 1992; Simo et al. 1993; Graziano 2000; Wissler et al. 2003; Föllmi et al. 2006; Basilone and Sulli 2018). The lower Bedoulian carbonate platforms of the Western Tethys are characterized by abundant rudist bivalves. The example described here provides an excellent opportunity to investigate the process of installation and evolution of a carbonate platform in a rift setting. Besides, it also represents a case-study of stromatoporoid development in Aptian deposits, a biofacies also described from the early Aptian by Schlagintweit and Rashidi (2022) in Central Iran, but more widely known from the Jurassic (Millán et al. 2011; Godet et al. 2011; Huck et al. 2011; Huck and Heimhofer 2015). They have also been described in the Valanginian of the Gulf of Mexico by Loucks et al. (2017), associated with barrier reef environments in a transgressive context.

Geological setting

The Prebetic (Fig. 1a) is characterized by the development of a carbonate platform that extends continually from the Tíscar Fault (province of Jaén, Fig. 1b) to Cabo de la Nao (province of Alicante; Fig. 1a). West of the Tíscar Fault, the Prebetic crops out in several isolated tectonic blocks that made up the Prebetic of Jaén (Vera 2004; Fig. 1b). The Sierra de Bedmar-Jódar is located in the Prebetic of Jaén (Martín-Chivelet et al. 2002, 2019; Vera 2004; Molina et al. 2012; Nieto et al. 2022; Fig. 1a, b); palaeogeographically, it belongs to the South Iberian Continental Margin (SICM; Fig. 1c). It is made up of several tectonically isolated outcrops, situated to the west of the Tíscar. Each isolated unit of the Prebetic of Jaén is part of the Betic thrust front and tectonically overlies the Neogene of the Guadalquivir Basin. The main thrusting phase of the Betic units has been dated as Burdigalian-Messinian, with a net tectonic displacement towards the N-NW and W (Sanz de Galdeano et al. 2013). The structure of the Sierra de Bedmar-Jódar is an anticline plunging to the NW; its southern flank shows an average dip of 45°, whereas the northern flank is subvertical or slightly reversed. The axis of the fold is convex to the NW-W, with an average strike of N30°E (Fig. 1d).

The oldest strata of the Sierra de Bedmar-Jódar unit are Valanginian marly limestones, marls and sandstones, with intercalated sandy dolostones (Molina et al. 2012; Ruiz-Ortiz et al. 2014). These lithofacies are part of the Los Villares Fm, assigned to the upper part of the lower Valanginian/lower part of upper Valanginian (Ruiz-Ortiz et al. 2014; Fig. 2). They are overlain by the carbonates of the Llopis Fm, studied here, which are dated as early Aptian (Molina et al. 2011, 2012; Nieto et al. 2012; Ruiz-Ortiz et al. 2014). The two lithostratigraphic units are separated by a hiatus that encompasses the Hauterivian and part of the Barremian (Molina et al. 2015, 2021; Fig. 2). The Upper Aptian Seguilí Fm overlies the Llopis Fm (Molina et al. 2015; Fig. 2). The boundary between these two formations does not crop out in the Sierra de Bedmar-Jódar. The Albian is represented by shallow platform limestones, locally dolomitized, from the Sácaras and Jumilla formations. The uppermost part of the succession is formed by massive dolostones attributed to the Caliza de Jaén Fm, deposited during the Cenomanian (Molina et al. 2015; Fig. 2).

Lithostratigraphy

This paper is focussed on the study of the shallow carbonate platform of the Middle Member (Mb) of the Llopis Fm. In the Prebetic of Alicante, where this unit was defined by Castro (1998) and Castro et al. (2008), this lithostratigraphic unit consists of three members: the lower member, composed of sandy limestones of the upper Barremian, the middle member, made of shallow platform limestones of the lower part of the lower Aptian, and the upper member, the "Agres bed", consisting of sandstones and sandy limestones of the lower Aptian (Fig. 2). In the Sierra de Bedmar-Jódar, the Middle Mb is made up of grey limestones of shallow-marine origin with rudists and stromatoporoids. In the present study area, the Seguilí Fm overlies the Llopis Fm, although the surface that separates both units does not crop out (Ruiz-Ortiz et al. 2014; Nieto

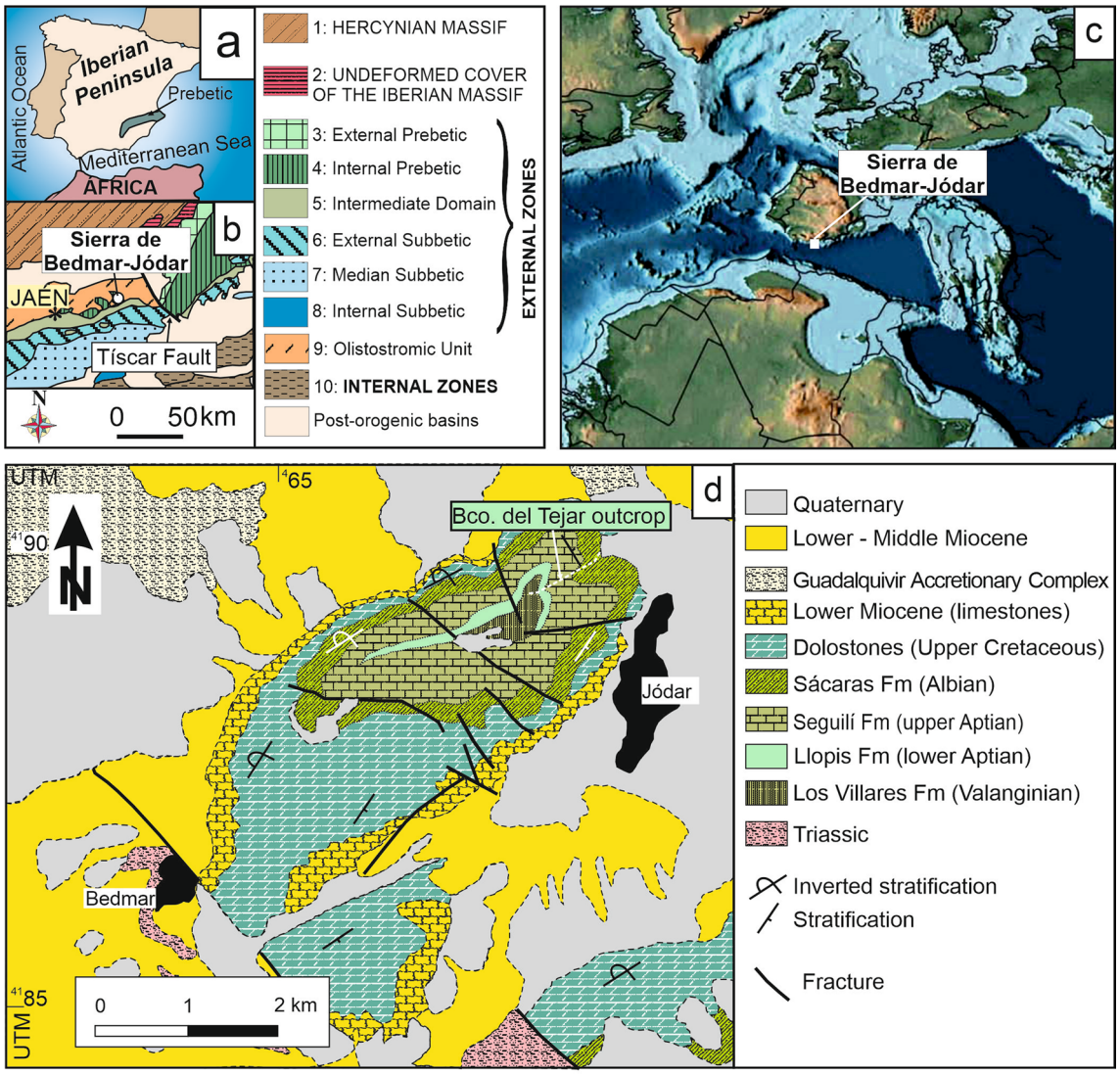

Fig. 1 **a** Location of the Prebetic (greenish-grey colour) in the Iberian Peninsula. **b** Geological sketch with location of the Sierra de Bedmar-Jódar, east of the city of Jaén. **c** Palaeogeography of the Western Tethys domain, from 120 Ma ago (Scotese 2016). **d** Simplified geological map of the Sierra de Bedmar-Jódar with location of the Barranco del Tejar outcrop

et al. 2022; Fig. 2). Laterally, towards the more internal (proximal) sectors of the Prebetic (i.e. the Sierra de Segura Unit), the Barremian-Albian interval is represented by a succession of shallow platform carbonate units that belong to the Arroyo de los Anchos Fm. Towards the more external (distal) sectors of the Prebetic (i.e. Mariola Unit, in the Prebetic of Alicante), where the Llopis Fm was defined, the lower Barremian is represented by the pelagic Los Villares Fm. The upper Barremian to lower Aptian is represented by the three members of the Llopis Fm. The hemipelagic Almadich Fm covers the lower–upper Aptian transition, and the upper Aptian to lower Cenomanian is represented by the succession of the Seguilí, Sácaras, Jumilla and Caliza de Jaén formations, composed mostly of shallow platform carbonates, with some terrigenous intervals (Fig. 2).

Methods

Nine stratigraphic sections have been studied amounting to a total thickness of 250 m, with detailed logging of biostratigraphy and facies, and the collection of 170 samples. Five sections (1–5) were logged across the top part of the outcrop (Fig. 3), whereas four sections (A–D) were studied in the ravine slope (Fig. 4). Thin-sections from the rock samples were used for petrographic and microfacies characterization, as well as for the identification of benthic

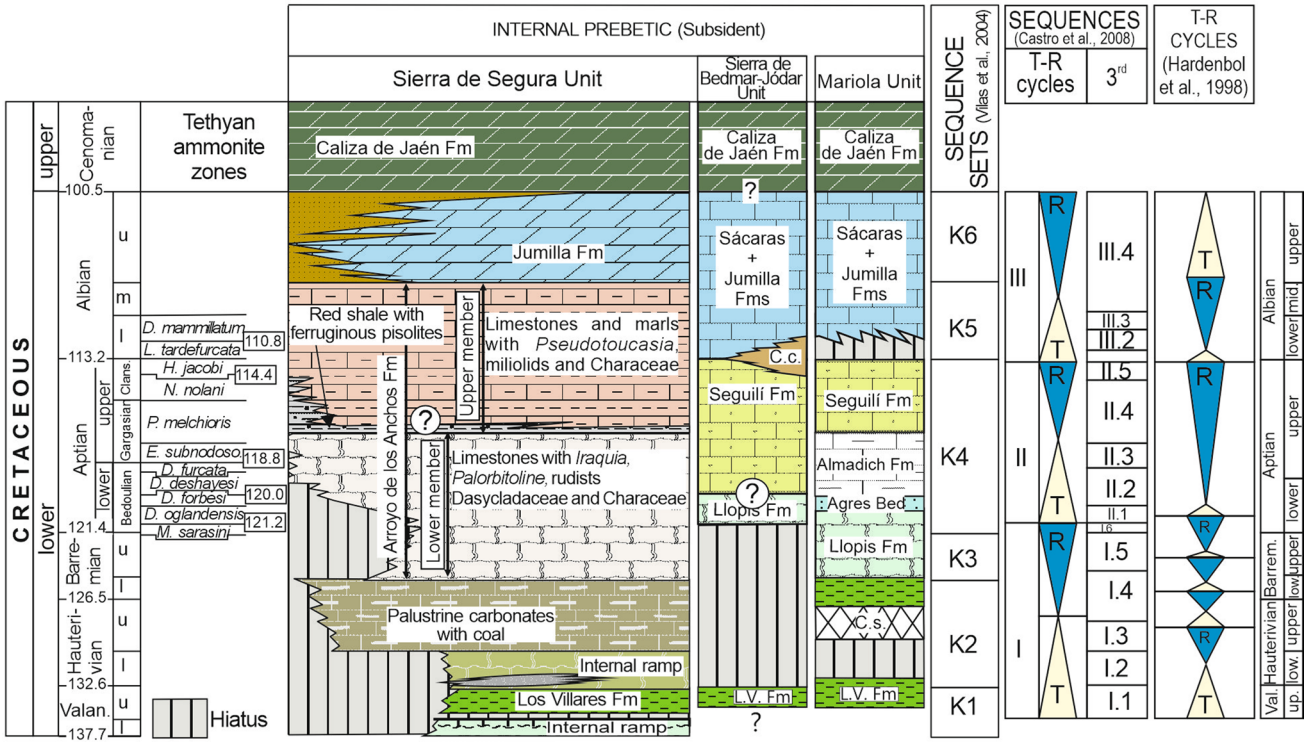

Fig. 2 Chronostratigraphic chart for the Prebetic of the Sierra de Segura and Mariola Units correlated with the chronostratigraphy of the Sierra de Bedmar-Jódar Unit. The numerical ages (in Ma) and the Tethyan Ammonite Zones from Gale et al. (2020). The sequence sets from Vilas et al. (2004) for the Early Cretaceous of Prebetic. The chronostratigraphic record of these units is correlated with the sequences (T-R cycles and sequences of 3rd order) from Castro et al. (2008) and the cycles of Hardenbol et al. (1998). Key to abbreviations: T-R: transgressive–regressive. C.c.: continental carbonates. C.s: condensed sediments. Fm: Formation. L.V. Fm: Los Villares Formation. Val: Valanginian. low./l: lower. mid./m: middle. up./u: upper

foraminifera, used for dating. The microfacies study was made using a Leica M205 C stereoscopic microscope. The average sampling interval was 1.47 m (250 m/170 samples), although the sampling intervals were variable. The size of sampling interval varied according to the thickness of beds or bed sets and was usually selected to sample each level, or, in the case of beds thicker than 1 m, to assess the variation between the lower and upper part of each. A facies map was made from the integration of field and microscopic observations (Fig. 5), using the satellite images from GoogleEarth Pro software.

Results

Biostratigraphy

The presence of two species of orbitolines, *Orbitolinopsis killiani* Henson and *Orbitolinopsis cuvillieri* Moullade, and the benthic foraminifer *Choffatella decipiens* Schlumberger in the present study area (Fig. 3) characterize the biostratigraphic unit 1 of Castro et al. (2001), as defined in the Prebetic of Alicante and dated as earliest Aptian (Bedoulian). The monopleurid rudist *Mathesia* sp. and requieniid *Toucasia* sp. have also been recognized, although they provide only a broad late Barremian to Albian age without further precision (Skelton and Gili 2012). The biostratigraphic unit 1 of Castro et al. (2001) was correlated with the nanoplankton biozone of *Hayesites irregularis*, and would be equivalent to the ammonite zones of *Deshayesites oglanlensis* and base of *Deshayesites forbesi* (Skelton et al. 2019). Above the Llopis Fm in the studied area, the Seguili Fm crops out. Nieto et al. (2018, 2022) recorded the presence in it of *Orbitolina (Mesorbitolina) texana* Roemer, dating this formation to the late Aptian. In summary, the Llopis Fm strata studied here can be attributed an early Aptian age, probably its earliest part.

Facies analysis

Six lithofacies associations (L1–L6) and twelve facies have been recognized (Table 1; Figs. 3, 4 and 5).

Lithofacies association 1 (L1): mixed quartz/carbonate sandstone with peloids and several kinds of bioclasts (Table 1). This lithology forms bodies of mounded geometry with

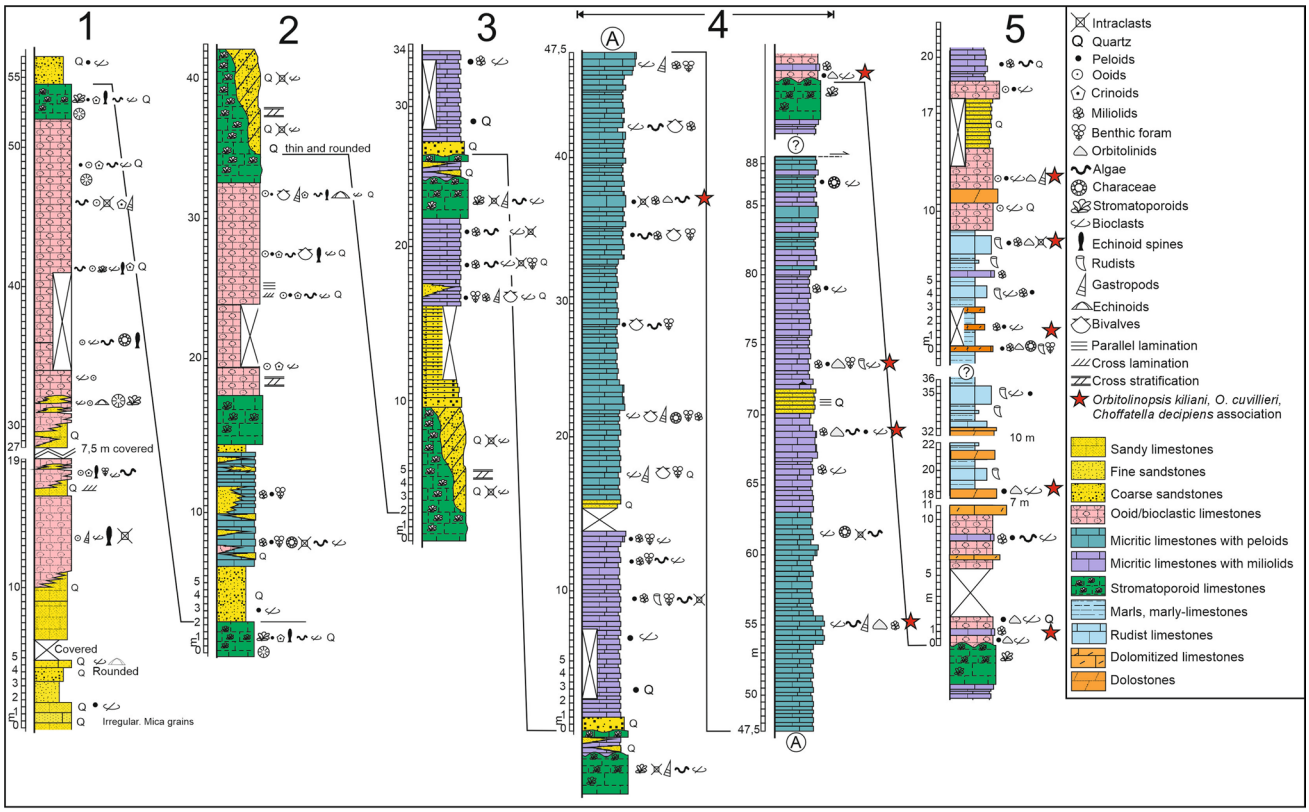

Fig. 3 Stratigraphic sections from the top transect of the Barranco del Tejar outcrop. The colour of the lithologies are equivalent to those shown in Figs. 4, 5 and 8

planar cross lamination. They are interpreted as having been deposited as sandy bars with grain-size fining-upwards; (microfacies 1A, Table 1; Figs. 6a, 7a and microfacies 1B, Table 1; Figs. 6b, 7b). There is a lateral change from L1 to L2 lithofacies (Table 1).

Lithofacies association 2 (L2): limestones with ooids, bioclasts and/or peloids. There are two microfacies, grainstone with ooids and/or bioclasts (microfacies 2A; Table 1; Figs. 6c, 7c) and grainstone with peloids (microfacies 2B; Table 1; Fig. 7d). As in lithofacies 1 (L1), these lithologies form oolitic bars with planar cross-lamination and cross-stratification, with a predominance of oolites (microfacies 2A) in the lower part of the sedimentary body and peloids (microfacies 2B) mainly present in the upper part (Fig. 7d).

Lithofacies association 3 (L3): limestone with peloids, bioclasts and charophytes. Two microfacies have been distinguished (Table 1): packstone with peloids and/or bioclasts (3A in Table 1; Figs. 6d, 7e) and mudstone, locally wackestone, with charophytes (3B in Table 1; Fig. 7f). In microfacies 3A, benthic forams (*Cuneolina* sp. and *Debarina* sp.), algae (*Salpingoporella* sp., *Bacinella* sp.) and orbitolines (*Orbitolinopsis killiani*, *O. cuvillieri*) have been identified. In microfacies 3B, *Atopochara trivolvis* and *Clavator grovesii* have been tentatively identified.

Lithofacies association 4 (L4): three microfacies have been recognised (Table 1). Microfacies 4A is wackestone with peloids and/or bioclasts. Microfacies 4B is wackestone with miliolids and 4C is mudstone, locally wackestone, with charophytes (Table 1; Fig. 7g).

Lithofacies association 5 (L5): rudist limestone (Table 1; Figs. 6e; 7h). Two lithofacies make up this association: a basal marly or marlstone unit, overlain by a floatstone unit with rudists (*Mathesia* sp., *Toucasia* sp.) and nerineid gastropods. The microfacies of the floatstone is mostly grainstone/packstone with ooids and bioclasts. The embedded rudists form decimeter-scale biostromes.

Lithofacies association 6 (L6): floatstone with stromatoporoids (Figs. 6f, 7i, j). This association is organized into bodies of metre-scale and lenticular morphology. At outcrop, the stromatoporoids are present in the form of bioherms and biostromes. Bioherms appear as individual mounds, whereas

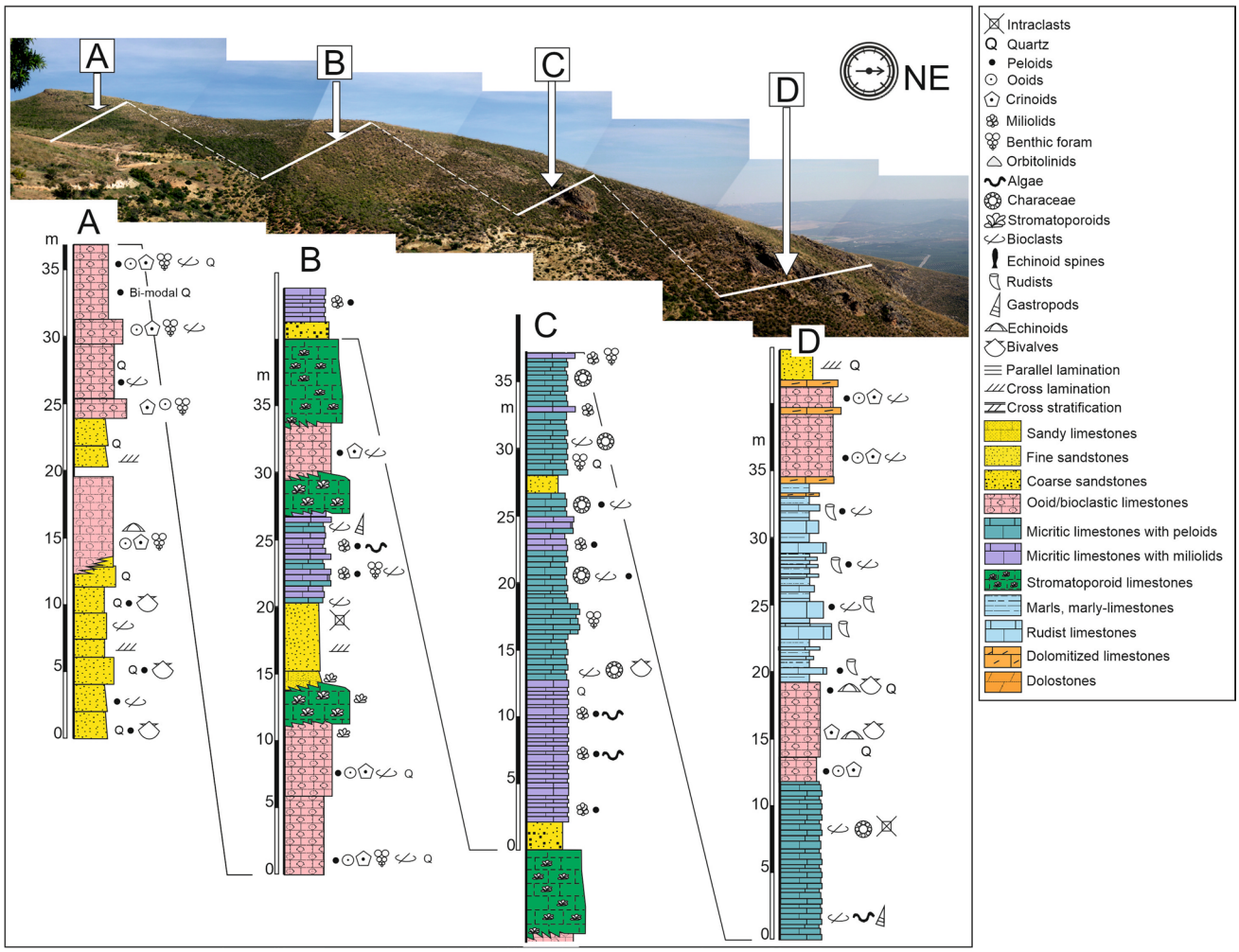

Fig. 4 Stratigraphic sections on the slope from the Barranco del Tejar. A panoramic view of the outcrop is shown above the stratigraphic columns indicating the location of each of the latter. The colour of the lithologies and the symbols of textural elements are equivalent to those shown in Fig. 3

biostromes have a larger lateral extent (100–200 m) (Fig. 5). The stromatoporoids are found in life position, embedded in a limestone matrix, strongly recrystallized and locally dolomitized, stained by Fe oxides. These stromatoporoid bodies show a locally staggered arrangement.

Facies 7, dolostones: these facies show an irregular distribution, interfingering with any of the previous lithofacies. The rhombohedral dolomite crystals are mainly developed in the micritic matrix, but are also observed in any of the above microfacies. They are late diagenetic related to deformational events of the orogenic phases (Table 1; Fig. 7f).

Sequence stratigraphic architecture

The lithofacies associations shown in Table 1 are organized into elemental sequences (ES) of decametre-scale that are repeated throughout the studied outcrop (Figs. 5, 8). The detailed sections (Figs. 3, 4) and facies map (Fig. 5), illustrate the lateral and vertical transitions between them. Analysis of the outcrops reveals that the general succession dips towards the E to NE, showing a geometry of sediment bodies prograding towards the E-NE. This differs from the general palaeogeographic trends in other platform areas of the SICM, where the main progradation direction is towards the SE (Castro 1998; Castro et al. 2008; Martín-Chivelet et al. 2019).

Each elemental sequence is determined according to the grouping of constituent lithofacies. Eight elemental sequences have been identified thereby (Fig. 8), and these can be grouped in three higher-scale sequences:

- Elemental sequences ES1 and ES2 (Fig. 8). The base of each elemental sequence is composed of sandstone with

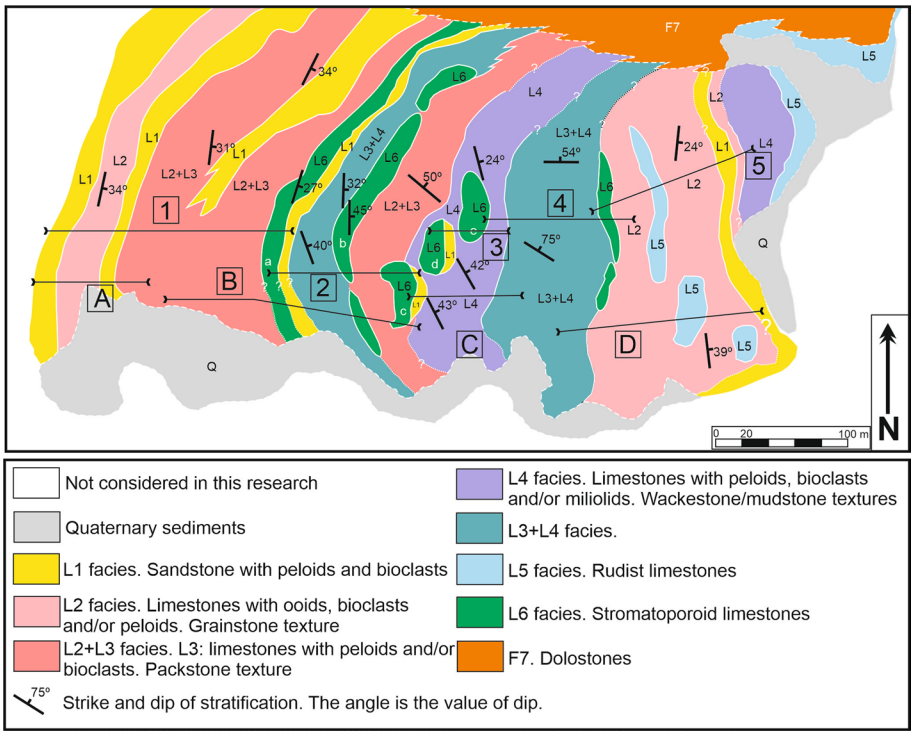

Fig. 5 Lithofacies map of the Llopis Fm in the Barranco del Tejar outcrops. The position of the different stratigraphic sections represented in Figs. 3 and 4 are indicated as 1 to 5 (Fig. 3) and A to D (Fig. 4). The colours are equivalent to those shown in Figs. 3 and 4

microfacies 1A or 1B (lithofacies association L1), which change laterally to type L2 lithofacies association (grainstone with ooids and/or bioclasts, 2A, and grainstone with peloids, 2B, Table 1). Both lithofacies associations developed under moderate energy environments, the first (L1) with a clear terrigenous influx and the second (L2) developed on a more open shallow platform, with wave influence, where the carbonate factory became well established. Both lithofacies associations probably record a transgressive trend (e.g. Castro et al. 2008; Bonvallet et al. 2019; Skelton et al. 2019). The ES2 (Fig. 8) shows the L3 lithofacies association overlying L2. The L3 lithofacies association probably developed in less energetic areas of the platform, with an eventual supra-tidal influence, as recorded by the presence of charophytes. The L3 association may mark the transition from a transgressive, to a highstand systems tract.

- Elemental sequences ES3, ES4, ES5 and ES6 (Fig. 8). Both the ES3 and ES4 again begin with the proximal L1 lithofacies association. In ES3, L1 is succeeded by lithofacies associations L2 and L3, recording shallow (moderately energetic) to locally supratidal conditions, most likely associated with the development of a coastal barrier in a transgressive context and the first stages of the highstand systems tract (L3). In the elemental sequence ES3, the L6 lithofacies association, with stromatoporoids, directly overlies L3 lithofacies marking the installation of an external, relatively deeper water barrier (Leinfelder et al. 2005).
- In the ES4, ES5 and ES6 (Fig. 8), L3 is succeeded by the L4 lithofacies association, interpreted to have been deposited in a lagoonal setting, with some local influx of freshwater, marked by the presence of microfacies 4C. This lithofacies association could be associated with highstand deposits (cf. Amodio et al. 2013). Finally, on top of L4 (Fig. 8), in the ES4, ES5 and ES6, stromatoporoid limestones (lithofacies association L6) appear, again presumed to represent a barrier between the lagoon and fully open platform conditions. This barrier must also have developed in the highstand phase. The irregular morphology at the top of stromatoporoid limestones can be interpreted as an erosive surface, probably related to subaerial exposure as a consequence of a drop in sea level.
- Elemental sequences ES7 and ES8 (Fig. 8). ES7 shows the development of rudist biostromes (with microfacies 5A) within a domain characterised by ooid bars and moderate energy waters, represented by facies association L2. Terrigenous influence must also be considered, given the presence of intercalated levels of marls and marly limestones (facies 5A). These elemental sequences are taken to be transgressive, possibly close to the onset of highstand conditions. The ES8 (Fig. 8) includes coastal barrier deposits with clastic influence (L1) as well as ooid bar development (L2). Both associations neighbour lagoonal facies (L4) which show evidence for freshwater influence close to the coastal barrier, but in more distal environments they are dominated by rudist assemblages

Table 1 Lithofacies associations and facies from the Barranco del Tejar outcrop, and interpreted sedimentary environments

No	Lithofacies associations	No	Facies	Textural features and sedimentary structures	Environment
L1	Sandstone with peloids and bioclasts	1A	Sandstone with coarse grains	Quartz and some peloids and/or bioclasts. Some samples show serpulids, bryozoan and clasts of stromatoporoids Planar cross lamination	Inner shallow platform with influence of waves
		1B	Sandstone with fine grains		
L2	Limestone with ooids, bioclasts and/or peloids	2A	Grainstone with ooids and/or bioclasts	Ooids, bioclasts, quartz, echinoderms, benthic foraminifera, gastropods, algae (*Salpingoporella* sp., *Triploporella* sp.), rudist bioclasts, corals, crinoids, bryozoans, stromatoporoids, micritized grains Planar cross—lamination and planar cross—bedding. Stylolites	Inner shallow platform—with moderate energy. This lithofacies laterally changes to sandstone facies (L1 lithofacies)
		2B	Grainstone with peloids	Peloids, intraclasts, orbitolines (*Orbitolinopsis killiani*, *O. cuvillieri*), miliolids, algae, echinoids, crinoids, quartz	
L3	Limestone with peloids, bioclasts and charophytes	3A	Packstone with peloids and/or bioclasts	Peloids, indeterminate bioclasts, algal bioclasts, rudist bioclasts, intraclasts, benthic foraminifera (*Cuneolina* sp., *Debarina* sp.), miliólids, algae (Dasycladaceae, *Salpingoporella* sp., *Bacinella* sp.), bivalves, stromatoporoids, orbitolines (*Orbitolinopsis killiani*, *O. cuvillieri*)	Shallow platform with low to moderate energy
		3B	Mudstone, locally wackestone with charophytes	Charophytes [*Atopochara trivolvis* (?), *Clavator grovesii* (?)], peloids, bioclasts	Supratidal environment with episodic freshwater influence
L4	Limestone with peloids, bioclasts miliolids and/or charophytes	4A	Wackestone with peloids and/or bioclasts	Peloids, indeterminate bioclasts, intraclasts, quartz, benthic foraminifera (*Pseudotextularia* sp., *Cuneolina*, sp., *Debarina* sp.), miliolids, gastropods, bivalves, stromatoporoid bioclasts	Very shallow lagoon, locally with freshwater inflows where charophytes were developed
		4B	Wackestone with miliolids	Miliolids, charophytes, peloids, bioclasts, quartz, orbitolines (*Orbitolinopsis killiani*, *O. cuvillieri*), *Debarina* sp., *Choffatella* sp., *Bacinella* sp.), rudist bioclasts	
		4C	Mudstone with charophytes	Charophytes [*Atopochara trivolvis* (?), *Clavator grovesii* (?)], peloids, bioclasts (gastropods, bivalves), algae (Dasycladaceae, *Triploporella* sp., *Pithonella* sp.)	
L5	Rudist limestone	5A	Marl or marlstone	Bioclasts of rudists	Lagoon with small rudist biostromes with episodic oolite flows
		5B	Floatstone with rudists with a grainstone/packstone texture. Small rudist biostromes	Rudists (*Mathesia* sp., *Toucasia* sp.), ooids, bioclasts, echinoids, gastropods, bryozoans, coarse grains of quartz	

Table 1 (continued)

No	Lithofacies associations	No	Facies		Textural features and sedimentary structures	Environment
L6	Stromatoporoid limestone	6	Floatstone with stromatoporoids; stromatoporoid biostromes		Stromatoporoids, peloids, echinoids, quartz, red algae, solitary corals, rudist bioclasts When colonial corals present, partially dolomitized	Barrier. High energy environment
		F7	Dolostone		The dolomitization has affected many lithofacies	

(lithofacies association L5; Fig. 6e) with less terrigenous input. Although no evidence can be seen at outcrop, it is possible that this lagoon was cut off from the open shelf by low rudist banks. Both L4 and L5 lithofacies associations would have developed under highstand conditions.

Depositional model

Lithofacies association L1, sandstone with peloids and bioclasts (Table 1), were deposited on an inner shallow platform where the action of the waves produced sand-wave sediment bodies (James and Dalrymple 2010; Fig. 9a). The microfacies 1A (sandstone with coarse grains) is considered more proximal with respect to microfacies 1B (sandstone with fine grains). The origin of the sands of this facies association should probably be sought on the hinterland. Towards more open-marine sectors, the L1 facies association gradually passes towards the limestones of L2 and L3 facies associations, deposited on a shallow platform environment (Flügel 2010; Fig. 9a, b). The L2 facies association consists of grainstones of two types, 2A presents ooids/bioclasts whereas type 2B is mainly composed of peloids. The ooidal type (2A) implies important tidal currents, forming ooid barrier island or shoals, being more energetic than the peloidal type 2B. Facies association L3, limestone with peloids, bioclasts and charophytes, consists of packstones (microfacies 3A), which are dominated by peloids and/or bioclasts, related to a more quiet and restricted part of the internal platform (Fig. 9a, b). Where the bioclasts dominate over the peloids, this facies is associated with an assemblage of benthic forams (*Cuneolina* and *Debarina*), dasycladacean algae (*Salpingoporella* and *Triploporella*) miliolids, nerineids and echinoids. Quartz is commonly present indicating a strong continental influence. In addition, this part of the platform must have been influenced by freshwater, responsible for the development of ponds in which charophytes proliferated (microfacies 3B), in a supratidal environment. The former facies delimit the lagoon (Fig. 9b), represented by limestones with L4 lithofacies (Reijmer 2021).

The lagoon was a low-energy shallow environment, episodically affected by currents providing thin oolitic or peloidal drifts (from L2 or L3 lithofacies associations), which are interfingered between the carbonates of L4 association (Table 1; Fig. 9b). Microfacies 4A (wackestone with peloids and/or bioclasts) and 4B (wackestone with miliolids), with micritic matrix and benthic microfauna were deposited in quieter environments, in a relatively deep lagoon, probably protected from the most energetic seawater by a barrier made up by stromatoporoids (Fig. 9b). The morphology of the stromatoporoid barrier varied over time: first, fairly continuous along the outcrop (biostromes) and, later, forming bioherms, apparently disconnected from each other (Fig. 5). In the lagoon, three sub-environments can be discerned. The

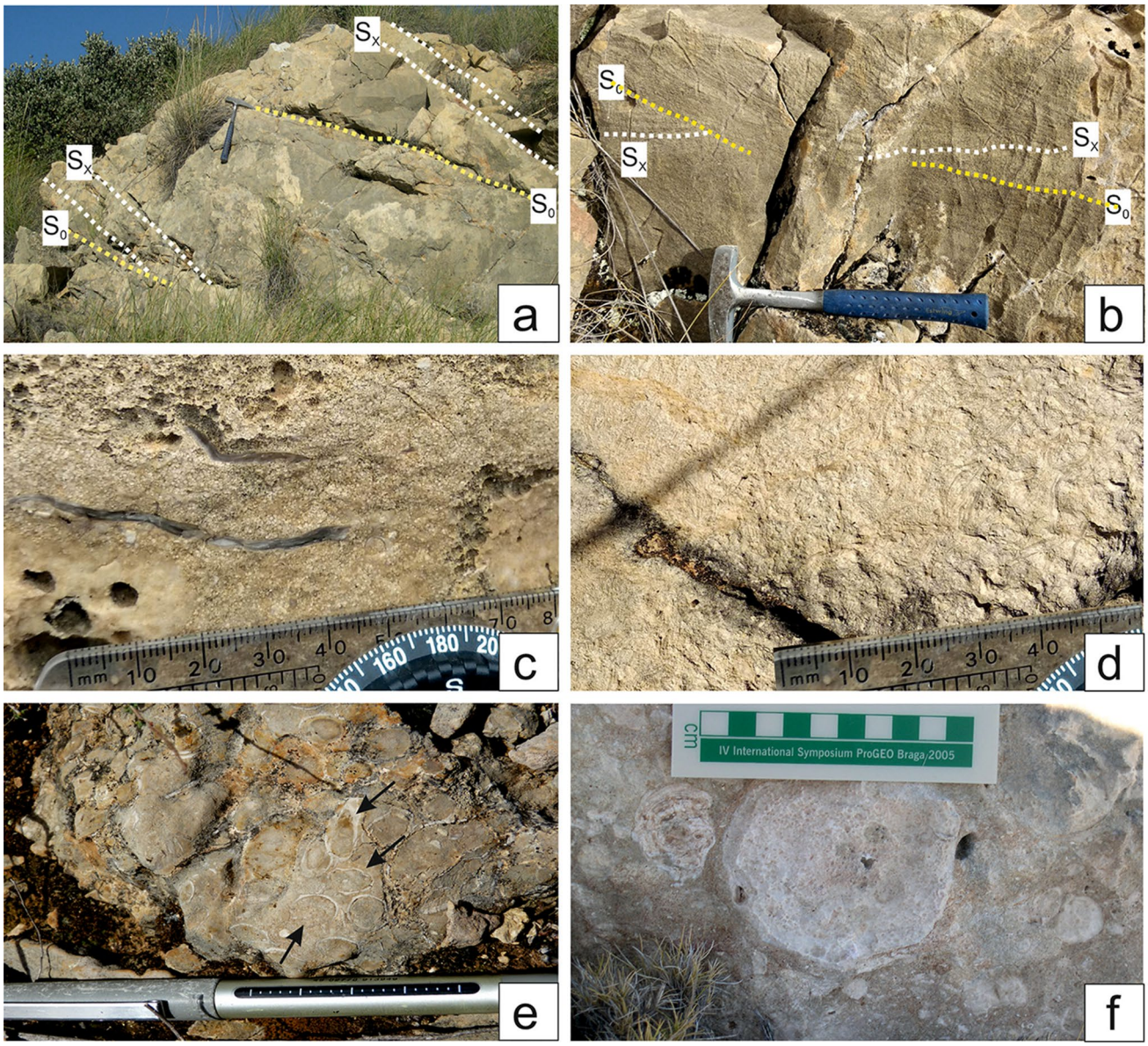

Fig. 6 Facies of Llopis Fm in the Barranco del Tejar outcrops. **a** Sandstone with coarse grains and planar-cross lamination, S_x (facies L1-1A, Table 1); S_0: stratification. **b** Sandstone with fine grains and planar-cross lamination (facies L1-1B, Table 1). **c** Limestone with ooids or peloids (facies L2-2A and 2B respectively, Table 1). **d** Limestone with bioclastic fragments, mainly bivalves (facies L3-3A, Table 1). **e** Rudist limestone, bouquet of *Mathesia* sp. (facies L5-5B, Table 1). The black arrows show some rudists (*Mathesia* sp.). **f** Stromatoporoid limestone (facies L6-6, Table 1)

one represented by microfacies 4A would be somewhat deeper than the environment where microfacies 4B (wackestone with miliolids) developed. An interesting feature of type 4B is the presence of the biosedimentary (calcimicrobial) structure *Bacinella* (Schlagintweit and Bover-Arnal 2013; Granier 2021). The shallowest of all, influenced by freshwater, would be represented by microfacies 4C (mudstone with charophytes).

Towards the proximal sectors the lagoon was limited by the carbonate sand bars (L2 lithofacies association), whereas towards the more open, external platform the limit of the lagoon was marked by bioconstructions of stromatoporoids (L6 lithofacies association; Table 1; Fig. 9b), which acted as relatively deep reefal barriers, in slightly deeper waters than those of the lagoon (Leinfelder et al. 2005). Stromatoporoids could grow in highly abrasive, energetic marine environments, and were tolerant to frequent reworking and redistribution, giving way to lateral accumulations (Leinfelder et al. 2005). The presence of erosive surfaces and thin iron crusts at the top of the stromatoporoid bioconstructions indicate

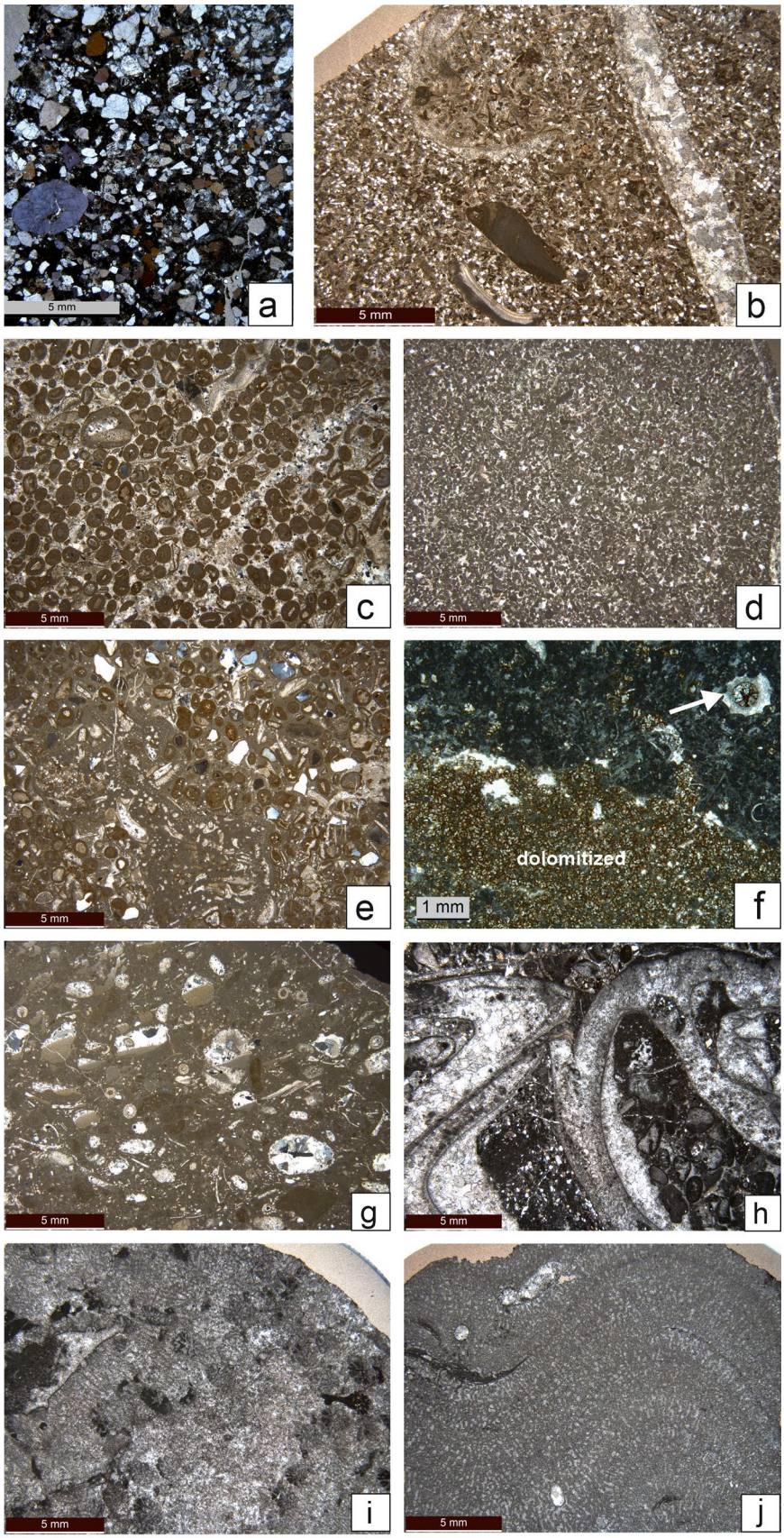

Fig. 7 Microfacies of the Llopis Fm from the Barranco del Tejar outcrops. **a** Sandstone with coarse grains, mainly quartz (microfacies 1A, Table 1). **b** Sandstone with fine grains, mainly quartz (microfacies 1B, Table 1). **c** Grainstone with ooids (microfacies 2A, Table 1). **d** Grainstone with peloids (microfacies 2B, Table 1). **e** Packstone with peloids; some have thin ooid coatings (microfacies 3A, Table 1). **f** Mudstone with charophytes, peloids and bioclasts partially dolomitized (microfacies 3B, Table 1). **g** Mudstone with charophytes and peloids (microfacies 4C, Table 1). **h** Grainstone and packstone with ooids, peloids and rudists (microfacies 5B, Table 1) **i** Floatstone with stromatoporoid (microfacies 6, Table 1). **j** Detail of internal structure of a stromatoporoid (microfacies 6, Table 1)

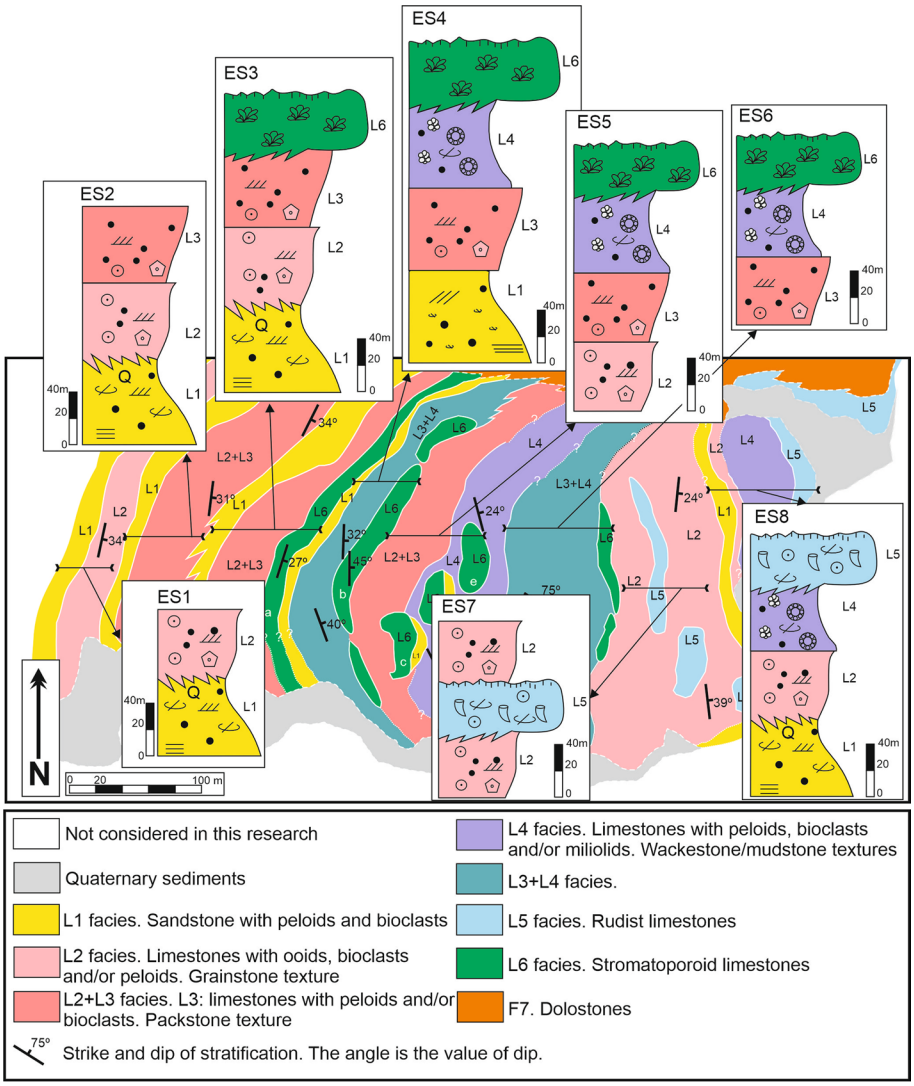

Fig. 8 Distribution of the elemental sequences (ES1 to ES8) in the facies map of the Barranco del Tejar outcrop. The colour and the symbols of textural elements are equivalent to those in Figs. 3, 4 and 5

that the growth of these bioconstructions was ended by an erosive phase, perhaps due to a higher wave energy, or relative sea-level falls, probably reaching occasional short-term emergence phases. The irregular surfaces on top of the bioconstructions are covered by sandstone beds (L1 lithofacies association).

The emergence of the rudist beds (L5 lithofacies association), coincident with the demise of stromatoporoids, can be related to a reduction in the input of terrigenous sands (lithofacies association L1), but with continued input of silty and carbonate materials, represented by facies 5A (marl or marlstone with bioclasts of rudists). Some rudist biostromes may have developed on this muddy substrate of the lagoon, represented by facies 5B (floatstone with rudists), occasionally affected by oolite drifts. Therefore, a change in the environmental conditions favouring carbonate production would eventually have led to the development of a shallower Urgonian-type carbonate platform with a shallow lagoon dominated by rudists (Fig. 9c). In view of the limited extent of the outcrop there are no data about the facies that would represent the border of the rudist-dominated lagoon in the upper half of the outcrop.

Discussion

Cyclicity and sedimentary evolution

From the detailed successions combined with the facies map (Figs. 3, 4 and 5) eight elemental sequences (ES1 to ES8, Fig. 8), in the sense of Catuneanu and Zecchin (2020), can be distinguished. These elemental sequences can be interpreted to represent three stages in the evolution of the platform (Fig. 9): a first stage, of installation of the platform (Fig. 9a); a second phase with early development of a lagoon-barrier system (Fig. 9b); and a third phase corresponding to a well-developed lagoon with rudists, that is, the development of an Urgonian-type Platform (Fig. 9c)

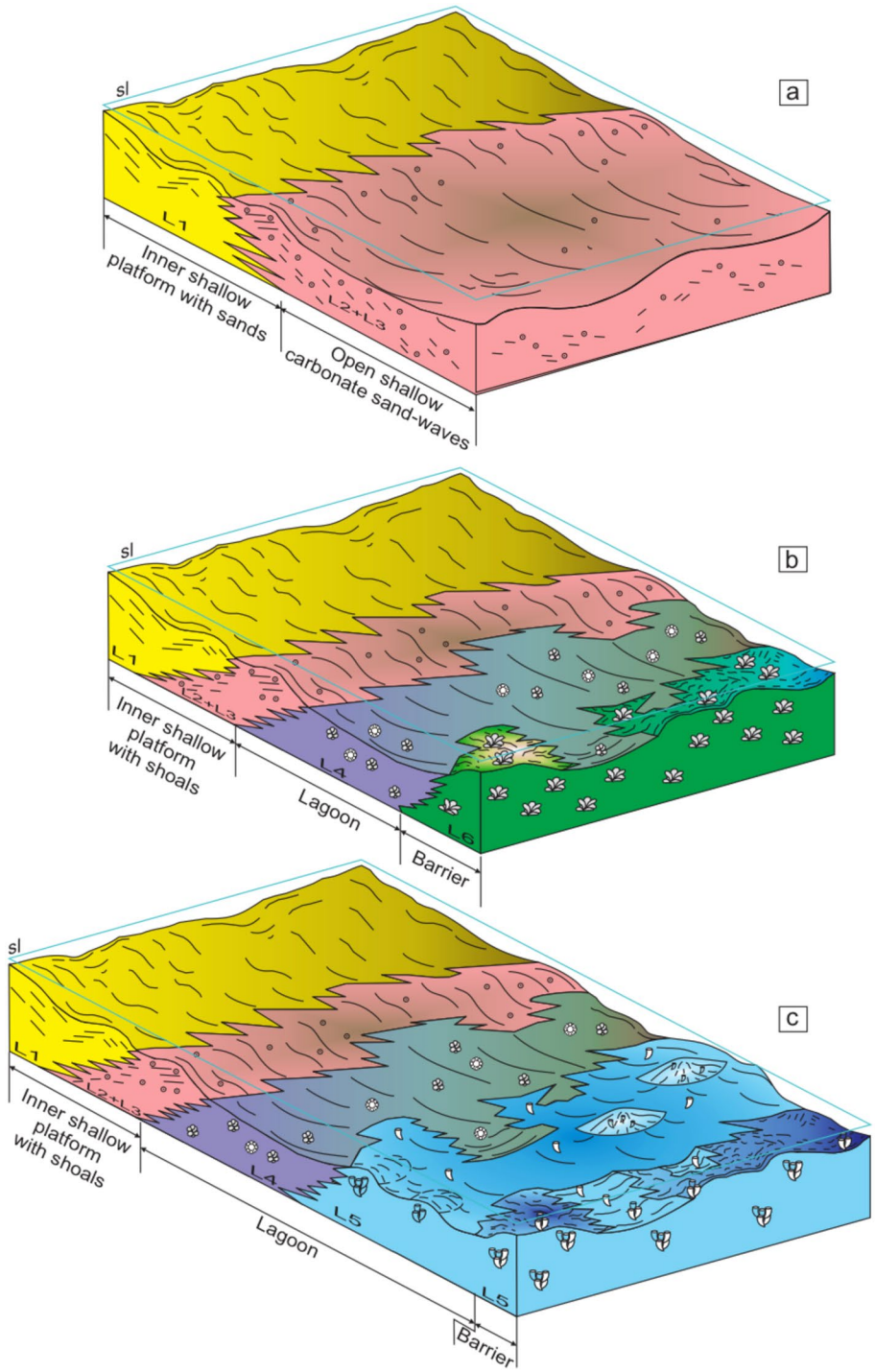

Fig. 9. 3D depositional models showing relations between lithofacies associations of Table 1 according to the stages of the evolution of the platform. **a** Installation of the shallow platform. **b** Development of a lagoon separated distally by a stromatoporoid barrier. **c** Establishment of an Urgonian-type platform with rudists. Diagrams not to scale

(e.g. Castro et al. 2008; Skelton and Gili 2012; Amodio et al. 2013; Masse and Fenerci-Masse 2013; Bonvallet et al. 2019; Skelton et al. 2019; Basilone 2021).

1. Installation of the platform (elemental sequences ES1 and ES2; Figs. 8, 9a). This stage is characterized by the predominance of high-energy siliciclastic (L1) and oolitic-peloidal (L2 + L3) facies, with the development of sand-waves, which separated a coastal environment from a more marine one. In the Prebetic, during the late Valanginian—earliest Aptian (Cycle I) each episode of carbonate platform progradation was preceded by the local sedimentation of siliciclastic units related to extensional tectonic pulses, leading to transgression stages (e.g. Castro et al. 2008; Martín-Chivelet et al. 2019). These extensional tectonic processes can be related to

the rotation of Iberia during the Barremian-Aptian (Bonvallet et al. 2019; Martín-Chivelet et al. 2019), closely connected with the opening of the Atlantic. As in the Helvetic shelf (Bonvallet et al. 2019), these extensional phenomena in the Prebetic would have given rise to differentiated tectonic blocks, rotated along listric faults, some of which would have become partially isolated from the rest of the shelf (Basilone and Sulli 2018; Basilone 2021). In addition to tectonic mechanisms, climatic conditions have also been invoked to explain the genesis of the siliciclastic sediments. Thus, Amodio et al. (2013) and Bonvallet et al. (2019) indicate that these deposits could be related to phases of strong continental weathering in warm, humid climatic conditions, similar to those suggested for the Southern Iberian Continental Margin (SICM) during the early Aptian (Aguado et al. 2014; Castro et al. 2019).

2. The early development of a lagoon-barrier system (ES3, ES4, ES5 and ES6; Figs. 8, 9b). As a consequence of extensional tectonics, subsiding domains developed and were filled by the deposition of lagoonal lithofacies (L4). They were bounded towards the inner shelf by ooid-peloidal bars (L2 + L3) and towards the outer part of the shelf by stromatoporoid bioconstructions (L6). Occasionally, both the bar and the lagoon may have been affected by freshwater influxes (facies 3B and 4C). This association of sedimentary environments can be interpreted as the consequence of rapid progradation of the shallow environments across the shelf (e.g. Castro et al. 2008). The presence of stromatoporoid bioconstructions is taken to reflect energetic conditions in barrier and inner shelf settings, associated with terrigenous inputs, as shown by the presence of quartz and abundant bioclasts in the L6 facies. Stromatoporoids develop particularly well in shallow, strongly erosive and possibly especially overheated water environments (Leinfelder et al. 2005). They have been linked to oligotrophic associations of organisms (Leinfelder et al. 2005; Bonvallet et al. 2019). At the top of the stromatoporoid bioconstructions are irregular surfaces that could be considered as erosional surfaces and, perhaps, with subaerial exposure, suggesting a drop in sea level that may have caused eventual emergence of the lagoon barrier. Given the tectonic and environmental conditions described in the previous section, these drops in relative sea level could be related either to tectonic pulses, or to environmental change which would have favoured renewed continental weathering, hence increase of siliciclastic influx, which would have spread over the erosive surface at the top of the bioconstructions.
3. A well-developed lagoon with rudists, leading to development of an Urgonian-type platform (ES7 and ES8; Figs. 8, 9c). Lithofacies association L5 denotes the establishment of a shallow-marine environment, relatively protected from wave action, but with a continental influence of lesser intensity than that associated with the development of lithofacies association L6, stromatoporoid limestones. This must have been an environment with well-oxygenated waters, where, in addition to rudists, echinoids, gastropods and bryozoans proliferated, with normal salinity and good communication with open shelf environments (Castro 1998; Castro et al. 2008; Skelton and Gili 2012; Martínez-Rodríguez et al. 2018; Skelton et al. 2019). These waters would originally have been sporadically turbid, with clays and nutrients issuing from the hinterland (facies 5A). As turbidity gradually decreased, rudists flourished in the lagoon giving rise to small biostromes. Although not observed in the outcrop of the study area, it is possible that the lagoon was bounded by rudist banks, from which shells and bioclasts were washed in by storm currents. The development of these environments would be consistent with a highstand context, favouring a productive carbonate factory. Meanwhile, the latter might also have been favoured by relatively warm but semi-arid to arid climatic conditions, reducing weathering rates on the continent (e.g. Skelton and Gili 2012; Bonvallet et al. 2019; Reijmer 2021).

From biostratigraphic data, the Llopis Fm in the Bedmar-Jódar Unit has been assigned to the lower part of the lower Aptian, without further precision. It could thus be correlated with the lower part of the K4 sequence of Vilas et al. (2004) (Fig. 2), characterised mainly by intense extensional tectonic activity, with block rotation, accounting for localised, non-simultaneous episodes of high sedimentation rates throughout the entire Prebetic platform, together with interruptions of sedimentation and important changes in thickness between neighbouring areas.

According to the sequences proposed by Castro et al. (2008), the Llopis Fm should be correlated with the lower part of his cycle II, specifically with the third-order sequence II.1, with a general transgressive–regressive trend. The platform installation (phase 1, Fig. 9a) and early stages of development of the stromatoporoid lagoon-barrier system (phase 2, Fig. 9b) identified herein could thus be correlated with the transgressive stage, whereas the development of a rudist-dominated lagoon (Fig. 9c), could then correlate with the base of the highstand stage (Castro et al. 2008).

By comparison with the T-R cycles proposed by Hardenbol et al. (1998), the third order cycle II.1 of Castro et al. (2008) would coincide with the regressive stage of Hardenbol et al. (1998) at the beginning of the Aptian and the succeeding transgressive stage. The phase 3 development of the Urgonian-type platform in the study area, would then correspond to the beginning of the major Aptian regressive cycle

of Hardenbol et al. (1998) (Fig. 2). The differences between these schemes could reflect the influence of the local tectonics that affected the Prebetic platform during the Aptian, giving rise to individualized blocks, partly disconnected from the continent and with their own, unique sequential histories.

Early Aptian palaeogeographic setting of the Sierra de Bedmar-Jódar Unit

The earliest Aptian development of the Prebetic carbonate platform in the Sierra de Bedmar-Jódar has unique features that can be interpreted as a result of the partial tectonic individualisation of a block within the broader Prebetic Platform. The tectonic individualisation was not total, since sediments clearly originating from the continent (L1) are recorded in this block (e.g. Molina et al. 2012; Ruiz-Ortiz et al. 2014; Nieto et al. 2022). The first of these stratigraphical singularities is that the Llopis Fm in the study area directly overlies the Los Villares Fm, the uppermost part of which has been assigned to the upper Valanginian (Molina et al. 2021). There is thus a hiatus between the two lithostratigraphic units encompassing the Hauterivian, Barremian and, possibly, the earliest part of the Aptian (Fig. 2). Coevally, in the more proximal sectors of the Sierra de Segura Unit (Fig. 2), different environments were established, ranging from internal ramp settings to carbonate palustrine environments with coal formation, over which a shallow Urgonian-type platform developed, equivalent to that developed in other parts of the Prebetic (García-Hernández et al. 2003). Meanwhile, in the Mariola Unit (Prebetic of Alicante), a discontinuous upper Valanginian-lower Barremian record of Los Villares pelagic facies was developed (Fig. 2), overlain by the open platform mixed carbonates of the lower member of the Llopis Fm (upper Barremian), predating the Urgonian-type carbonate platform of the middle member of the Llopis Fm (Fig. 2; Castro et al. 2008; Vera 2004; Martín-Chivelet et al. 2019; Skelton et al. 2019; Martínez-Rodríguez et al. 2018). The latter sedimentary evolution is more similar to that recorded in other peri-Tethyan domains (e.g. Stein et al. 2012; Amodio et al. 2013; Bonvallet et al. 2019; Basilone 2021).

Another significant feature of the Sierra de Bedmar-Jódar is the presence of stromatoporoid facies (L6), which are not recorded in equivalent sections of the Sierra de Segura or the Prebetic of Alicante. These facies, common in Jurassic platforms generally (e.g. Leinfelder et al. 2005), characterize the stages before the Urgonian-type platforms were installed; these phases are characterized by a gradual reduction of the continental influence and, simultaneously, the development of the carbonate factory, which culminated in the development of the rudist facies.

The direct superposition of the carbonates of the Seguilí Fm (which were also deposited in a shallow carbonate platform during the late Aptian) over those of the Llopis Fm, studied in this paper, is another important feature of the Prebetic unit studied here. In the Sierra de Segura Unit, the Urgonian-type platform recorded by the lower member of Arroyo de los Anchos Fm (Fig. 2), has been considered to have developed in a transgressive context (García-Hernández et al. 2003). Meanwhile, in the Mariola Unit the upper member of the Llopis Fm (Agres Bed; Castro 1998; Castro et al. 2008) records the drowning of the carbonate platform and the beginning of hemipelagic sedimentation of the Almadich Fm, in which OAE 1a has been recorded (Castro et al. 2021). Neither the demise of the Llopis Fm platform nor the OAE 1a have been recorded in the Sierra de Bedmar-Jódar. On the contrary, there appears to be continuity between the Llopis Fm platform and the platform corresponding to the Seguilí Fm, which extends to the upper Aptian (Fig. 2). The tectonic control of sedimentation on the latter shelf continued to be important, especially in its final phase, which led to its demise (Nieto et al. 2022).

Conclusions

The lower Aptian Llopis Fm shallow platform succession cropping out in the Sierra de Bedmar-Jódar, has been investigated by reference to nine high-resolution stratigraphic sections and a detailed facies map to reveal the facies architecture of this sector of the platform.

Six lithofacies associations have been distinguished, one siliciclastic-dominated (L1), five comprising carbonate facies associations (L2–L6), ranging from grainstones (2A, 2B), packstones (3A), wackestones (4A; 4B) and mudstones (3B, 4C, 5A), to floatstones (5B, 6), the last two characterized respectively by abundant macrofossils of stromatoporoids (L6), and rudists (5A, 5B). Finally, a late diagenetic dolomitic facies (F7) is recorded related to an advanced stage in the orogenic evolution of the region.

Lithofacies associations L1 to L6 are organized into eight successive elemental sequences, each interpreted as shallowing upward, and all developed in a very shallow carbonate platform-lagoon limited shoreward by clastic/ooid bars, and passing seaward either to stromatoporoid bioconstructions (bioherms and biostromes) or rudist biostromes. At the top of each of these sequences some features reveal shallowing with probable emergence, overlain by coastal bar deposits. Collectively, the successive elemental sequences demonstrate a progradational character, showing the growth of the platform towards the east.

The vertical succession of the elemental sequences defined in the studied platform allows the identification of three phases in the development of the platform, controlled by extensional tectonics together with influences from changes in climate:

(1) installation of the shallow platform in a transgressive context, as a result of tectonics and warm, humid climatic conditions;
(2) development of a lagoon separated distally by a stromatoporoid barrier, probably in the first stages of a relative sea-level highstand, but with falls of relative sea-level registered at the tops of the stromatoporoid bioconstructions, resulting from tectonic pulses;
(3) eventual establishment of an Urgonian platform dominated by rudists during a relative sea-level highstand, with optimal climatic conditions for the development of the carbonate factory.

During the early Aptian, the Bedmar-Jódar platform was likely isolated or partially isolated from the rest of the Prebetic platform, with progradation towards the NE, in contrast to the usual progradation to the SE or S shown in the Prebetic platform elsewhere. The sedimentation was mainly controlled by extensional tectonics, favouring sporadic emergence and tilting of the platform block so as to produce a different orientation of progradation. Occasional terrigenous influx from the continent and the presence of *Characeae* indicate freshwater inputs.

Acknowledgements Our acknowledgement to Antonio Piedra-Martínez, Technician of the Laboratory of Geology (University of Jaén). The comments of the reviewers and the Editor-in-chief of this Journal, Professor M. Tucker, have greatly improved the manuscript.

Author Contributions RMR, LMN, JMC, GAdeG, JMM, PARO: investigation, writing, review. RMR, LMN: editing and supervision. PWS: review, editing and supervision.

Funding Funding for open access publishing: Universidad de Jaén/CBUA. This research was funded by Project CGL2014-55274-P (Secretaría de Estado de I+D+i, Spain) and by the Research Group RNM-200 (Junta de Andalucía). RMR was funded by a PhD scholarship from the University of Jaén.

Data availability All the data necessary for the preparation of this paper are included in it. There is no supplementary data.

Declarations

Conflict of interest The authors declare that they have not conflict of interest.

References

Aguado R, de Gea GA, Castro JM, O'Dogherty L, Quijano ML, Naafs BDA, Pancost RD (2014) Late Barremian–early Aptian dark facies of the Subbetic (Betic Cordillera, southern Spain): Calcareous nannofossil quantitative analyses, chemostratigraphy and palaeoceanographic reconstructions. Palaeogeogr Palaeoclimatol Palaeoecol 395:198–221

Amodio S, Ferreri V, D'Argenio B (2013) Cyclostratigraphy and chronostratigraphy correlations in the Barremian-Aptian shallow-marine carbonates of the central-southern Apennines (Italy). Cretac Res 44:132–156

Basilone L (2021) Synsedimentary tectonics vs paleoclimate changes across the Aptian-Albian boundary along the Southern Tethyan margin: The panormide carbonate platform case history (NW Sicily). Mar Pet Geol 124:104801. https://doi.org/10.1016/j.marpetgeo.2020.104801

Basilone L, Sulli A (2018) Basin analysis in the Southern Tethyan margin: Facies sequences, stratal pattern and subsidence history highlight extension-to-inversion processes in the Cretaceous panormide carbonate platform (NW Sicily). Sed Geol 363:235–251. https://doi.org/10.1016/j.sedgeo.2017.11.013

Bonvallet L, Arnaud-Vanneau A, Arnaud H, Adatte T, Spangenberg JE, Stein M, Godet A, Föllmi KB (2019) Evolution of the Urgonian shallow-water carbonate platform on the Helvetic shelf during the late Early Cretaceous. Sed Geol 387:18–56

Bosence D (2005) A genetic classification of carbonate platforms based on their basinal and tectonic settings in the Cenozoic. Sed Geol 175:49–72. https://doi.org/10.1016/j.sedgeo.2004.12.030

Castro JM (1998) Las plataformas del Valanginiense superior-Albiense superior en el Prebético de Alicante. PhD Thesis, University of Granada

Castro JM, Ruiz-Ortiz PA (1995) Early Cretaceous evolution of the Prebetic zone in northeast Alicante province: the Sierra de Seguili section. Cretac Res 16:573–598

Castro JM, Company M, de Gea GA, Aguado R (2001) Biostratigraphy of the Aptian– Middle Cenomanian platform to basin domain in the Prebetic Zone of Alicante SE Spain: Calibration between Shallow Water Benthic and Pelagic Scales. Cretac Res 22:145–156. https://doi.org/10.1006/cres.2000.0249

Castro JM, de Gea GA, Ruiz-Ortiz PA, Nieto LM (2008) Development of carbonate platforms on an extensional (rifted) margin: the Valanginian-Albian record of the Prebetic of Alicante (SE Spain). Cretac Res 29:848–860

Castro JM, de Gea GA, Quijano ML, Aguado R, Froehner S, Naafs BDA, Pancost RD (2019) Complex and protracted environmental and ecological perturbations during OAE 1a – Evidence from an expanded pelagic section from south Spain (Western Tethys). Glob Planet Change 183:103030. https://doi.org/10.1016/j.gloplacha.2019.103030

Castro JM, Ruiz-Ortiz PA, de Gea GA, Aguado R, Jarvis I, Weissert H, Molina JM, Nieto LM, Pancost RD, Quijano ML, Reolid M, Skelton PW, López-Rodríguez C, Martínez-Rodríguez R (2021) High-resolution C-isotope, TOC and biostratigraphic records of OAE 1a (Aptian) from an expanded hemipelagic cored succession, Western Tethys: a new stratigraphic reference for global correlation and paleoenvironmental reconstruction. Palaeogeogr Palaeoclimatol 36:e2020PA004004. https://doi.org/10.1029/2020PA004004

Catuneanu O, Zecchin M (2020) Parasequences: Allostratigraphic misfits in sequence stratigraphy. Earth-Sci Rev 208:103289. https://doi.org/10.1016/j.earscirev.2020.103289

Clavel B, Conrad MA, Busnardo R, Charollais J, Granier B (2013) Mapping the rise and demise of Urgonian platforms (Late

Hauterivian-Early Aptian) in southeastern France and the Swiss Jura. Cretac Res 39:29–46
Eberli GP, Ginsburg RN (1989) Cenozoic progradation of northwestern Great Bahama Bank, a record of lateral platform growth and sea-level fluctuations. In: Crevello PD, Wilson JL, Sarg JF, Read JF (eds) Controls on carbonate platforms and basin development. SEPM Special Publication 44, p. 339–351
Enos P, Moore CH (1983) Fore-reef slope environment. Am Assoc Pet Geol Mem 33:507–537
Flügel E (2010) Microfacies of carbonate rocks—analysis, interpretation and application. Springer, Berlin
Föllmi KB (2012) Early Cretaceous life, climate and anoxia. Cretac Res 35:230–257. https://doi.org/10.1016/j.cretres.2011.12.005
Föllmi KB, Godet A, Bodin S, Linder P (2006) Interactions between environmental change and shallow water carbonate buildup along the northern Tethyan margin and their impact on the Early Cretaceous carbon isotope record. Paleoceanography 21:PA4211. https://doi.org/10.1029/2006PA001313
Gale AS, Mutterlose J, Batenburg S, Gradstein FM, Agterberg FP, Ogg JG, Petrizzo MR (2020) The Cretaceous period. In: Gradstein FM, Ogg JG, Schmitz MD, Ogg GM (eds) Geologic Time Scale, vol 2. Elsevier, Amsterdam, pp 1023–1086
García-Hernández M, Castro JM, Nieto LM (2003) La transgresión Aptiense en la Sierra de Segura (Zona Prebética, provincia de Jaén). Geogaceta 33:127–129
García-Mondéjar J (1990) The Aptian-Albian carbonate episode of the Basque-Cantabrian Basin (northern Spain): general characteristics, controls and evolution. In: Tucker ME, Wilson JL, Crevello PD, Sarg JR, Read JF (eds) Carbonate platforms: facies, sequences and evolution. IAS Special Publication, vol. 9, p. 257–290
Godet A, Föllmi KB, Stille P, Bodin S, Matera V, Adatte T (2011) Reconciling strontium-isotope and K-Ar ages with biostratigraphy: the case of the Urgonian plat- form, Early Cretaceous of the Jura Mountains, Western Switzerland. Swiss J Geosci 104:147–160
Granier BRC (2021) *Bacinella*, a discrete type of Mesozoic calcimicrobial structure. Carnets Geol 21:1–25
Graziano R (2000) The Aptian-Albian of the Apulia Carbonate Platform (Gargano Promontory, southern Italy): evidence of palaeoceanographic and tectonic controls on the stratigraphic architecture of the platform margin. Cretac Res 21:107–126
Hardenbol J, Thierry J, Farley MB, Jacquin T, de Graciansky PC, Vail PR (1998) Mesozoic and Cenozoic sequence chronostratigraphic framework of European Basins. In: de Graciansky PC, Hardenbol J, Jacquin T, Vail PR (eds) Mesozoic and Cenozic Sequence Stratigraphy of European Basins. SEPM 60, p 3–13
Hay WW, DeConto RM, de Boer P et al (2019) Possible solutions to several enigmas of Cretaceous climate. Int J Earth Sci 108:587–620. https://doi.org/10.1007/s00531-018-1670-2
Huck S, Heimhofer U (2015) Improving shallow-water carbonate chemostratigraphy by means of rudist bivalve sclerochemistry. Geochem Geophys Geosyst 16:5988. https://doi.org/10.1002/2015GC005988
Huck S, Heimhofer U, Rameil N, Bodin S, Immenhauser A (2011) Strontium and carbon-isotope chronostratigraphy of Barremian-Aptian shoal-water carbonates: Northern Tethyan platform drowning predates OAE 1a. Earth Planet Sci Lett 304:547–558
James PN, Dalrymple WD (2010) Facies models 4. Geological Association of Canada
Kiessling W, Flügel E, Golonka J (2003) Patterns of Phanerozoic carbonate platform sedimentation. Lethaia 36:195–225
Leinfelder RR, Schlagintweit F, Werner W, Ebli O, Nose M, Schmid DU, Hughes GW (2005) Significance of stromatoporoids in Jurassic reefs and carbonate platforms-concepts and implications. Facies 51:287–325. https://doi.org/10.1007/s10347-005-0055-8
Loucks RG, Kerans Ch, Zeng H, Sullivan PA (2017) Documenta5tion and characterization of the Lower Cretaceous (Valanginian) Calvin and Winn carbonate shelves and shelf margins, onshore north-central Gulf of Mexico. AAPG Bull 101:110–142. https://doi.org/10.1306/06281615248
Martín-Chivelet J, Berasategui X, Rosales I, Vilas L, Vera JA, Caus E, Gráfe KU, Mas R, Puig C, Segura M, Robles S, Floquet M, Quesada S, Ruiz-Ortiz PA, Frenegal-Martínez MA, Salas R, García A, Martín-Algarra A, Arias C, Meléndez M, Chacón B, Molina JM, Sanz JL, Castro JM, García-Hernández M, Carenas B, García-Hidalgo J, Gil J, Ortega F (2002) Cretaceous. In: Gibbons W, Moreno T (eds) The geology of Spain. Geological Society, London, pp 255–292
Martín-Chivelet J, López-Gómez J, Aguado R, Arias C, Arribas J, Arribas ME, Aurell M, Bádenas B, Benito MI, Bover-Arnal T, Casas-Sainz A, Castro JM, Coruña F, de Gea GA, Fornós JJ, Fregenal-Martínez M, García-Senz J, Garófano D, Gelabert B, Giménez J, González-Acebrón L, Guimerà J, Liesa CL, Mas R, Meléndez N, Molina JM, Muñoz JA, Navarrete R, Nebot M, Nieto LM, Omodeo-Salé S, Pedrera A, Peropadre C, Quijada IE, Quijano ML, Reolid M, Robador A, Rodríguez-López JP, Rodríguez-Perea A, Rosales I, Ruiz-Ortiz PA, Sàbat F, Salas R, Soria AR, Suarez-Gonzalez P, Vilas L (2019) The late Jurassic – early Cretaceous Rifting. In: Quesada C, C, Oliveira JT, (eds) The geology of Iberia: a geodynamic approach. Regional geology reviews. Springer, Cham
Martínez-Rodríguez R, Castro JM, de Gea GA, Nieto LM, Reolid M, Ruiz-Ortiz PA (2018) Facies analysis and stratigraphy of a lower Aptian Carbonate Platform section (Prebetic, Alicante, Spain). Geogaceta 64:31–34
Masse JP, Fenerci-Masse M (2013) Bioevents and palaeoenvironmental changes in carbonate platforms: the record of Barremian "Urgonian" limestones of SE France. Palaeogeogr Palaeoclimatol Palaeoecol 386:637–651. https://doi.org/10.1016/j.palaeo.2013.06.029
Masse JP, Borgomano J, Al Maskiry S (1998) A platform-to basin transition for lower Aptian carbonates (Shuaiba Formation) of the northeastern Jebel Akhdar (Sultanate of Oman). Sed Geol 119:297–309. https://doi.org/10.1016/S0037-0738(98)00068-2
Michalik J (1994) Lower Cretaceous carbonate platform facies, western Carpathians. Palaeogeogr Palaeoclimatol Palaeoecol 111:263–277
Millán MI, Weissert HJ, Owen H, Fernandez-Mendiola PA, Garcia-Mondéjar J (2011) The Madotz Urgonian platform (Aralar, northern Spain): palaeoecological changes in response to Early Aptian global environmental events. Palaeogeogr Palaeoclimatol Palaeoecol 312:167–180
Molina JM, Nieto LM, Ruiz-Ortiz PA, Castro JM, de Gea GA (2012) El Cretácico Inferior de la Sierra de Jódar-Bedmar (Prebético de Jaén, Cordillera Bética): facies, bioestratigrafía e interpretación paleoambiental. Geogaceta 52:73–76
Molina JM, Nieto LM, Ruiz-Ortiz PA, Castro JM, de Gea GA (2015) Secuencias deposicionales marinas someras con estromatopóridos (Aptiense inferior, Prebético, Sierra de Bedmar-Jódar). Geogaceta 57:79–82
Molina JM, Castro JM, de Gea GA, Nieto LM, Ruiz-Ortiz PA (2011) Aptian sedimentation related with a syn-rift episode: facies, biostratigraphy and paleoenvironmental interpretation (Prebetic of Jaén, Betic Cordillera, Spain). In: Bádenas B, Aurell M, Alonso-Zarza AM (eds) 28th IAS Meeting of Sedimentology, Zaragoza, Spain, Abstracts, p 497
Molina JM, Jiménez de Cisneros C, Nieto LM, Ruiz-Ortiz PA, Castro JM, de Gea, GA, Company M (2021) Emersión de una plataforma carbonatada aislada. Un ejemplo en el Prebético de Jaén (Hauteriviense-Barremiense, Zonas Externas Béticas). X Congreso Español de Geología, Abstract, 140

Najarro M, Rosales I, Martín-Chivelet J (2011) Major palaeoenvironmental perturbation in an early Aptian carbonate platform: Prelude of the Oceanic Anoxic Event 1a? Sed Geol 235:50–71

Nieto LM, Molina J-O, PA, Castro JM, de Gea GA, (2012) Ciclos de somerización en un lagoon de baja energía (Aptiense de la Sierra de Jódar, Prebético de Jaén. Cordillera Bética). Geotemas 13:83–87

Nieto LM, Reolid M, Rodríguez-Tovar FJ, Castro JM, Molina JM, Ruiz-Ortiz PA (2018) An integrated analysis (microfacies and ichnology) of a shallow carbonate-platform succession: upper Aptian, Lower Cretaceous. Betic Cordillera Facies 64:4. https://doi.org/10.1007/s10347-017-0515-y

Nieto LM, Molina JM, Ruiz-Ortiz PA, Castro JM, Reolid M, de Gea GA (2022) Palustrine sediments between two isolated shallow carbonate platforms (Aptian–Albian Transition, Prebetic of Jaén, South Spain). Minerals 12:116. https://doi.org/10.3390/min12020116

Philip J (2003) Peri-Tethyan neritic carbonate areas: distribution through time and driving factors. Palaeogeogr Palaeoclimatol Palaeoecol 196:19–37. https://doi.org/10.1016/S0031-0182(03)00311-0

Philip J, Masse JP, Camoin G (1995) Tethyan carbonate platforms. In: Nairn AEM, Ricou LE, Vrielynck B, Dercourt J (eds) The Tethys Ocean. Springer, Boston

Reijmer JJG (2021) Marine carbonate factories: review and update. Sedimentology 68:1729–1796. https://doi.org/10.1111/sed.12878

Ruiz-Ortiz PA, Castro JM (1998) Carbonate depositional sequences in shallow to hemipelagic platform deposits; Aptian, Prebetic of Alicante (SE Spain). Bull Soc Géol France 169:21–33

Ruiz-Ortiz PA, de Gea GA, Castro JM, García-García F, Molina JM, Nieto LM (2014) Datos y reflexiones para la reconstrucción paleogeográfica de un sector centro-septentrional (entre Bedmar y Jaén) de la Cordillera Bética durante el Cretácico Inferior. Rev Soc Geol España 27:111–126

Sanz de Galdeano C, García-Tortosa FJ, Peláez JA (2013) Estructura del Prebético de Jaén (sector de Bedmar). Su relación con el avance del Subbético y con fallas en el basamento. Rev Soc Geol España 26:55–68

Schlager W (1992) Sedimentology and sequence stratigraphy of reefs and carbonate platforms. American Association of Petroleum Geologists, Continuing Education Course Notes Series 34

Schlagintweit F, Bover-Arnal T (2013) Remarks on *Bačinella* Radoičić, 1959 (type species *B. irregularis*) and its representatives. Facies 59:59–73. https://doi.org/10.1007/s10347-012-0309-1

Schlagintweit F, Rashidi K (2022) The *"Orbitolina Limestone"* of central Iran: new data about microfacies, orbitolinid biostratigraphy, and palaeogeography. Facies 68:10. https://doi.org/10.1007/s10347-022-00647-2

Scotese CR (2016) PALEOMAP PaleoAtlas for GPlates and the PaleoData Plotter Program, PALEOMAP Project, http://www.earthbyte.org/paleomap-paleoatlas-for-gplates

Simo JA, Scott RW, Masse JP (1993) Cretaceous carbonate platforms: an overview. In: Simo JA, Scott RW, Masse JP (eds) Cretaceous Carbonate Platforms. American Association of Petroleum Geologists Memoir 56, p 1–14

Skelton PW, Gili E (2012) Rudists and carbonate platforms in the Aptian: a case study on biotic interactions with ocean chemistry and climate. Sedimentology 59:81–117. https://doi.org/10.1111/j.1365-3091.2011.01292.x

Skelton PW, Castro JM, Ruiz-Ortiz PA (2019) Aptian carbonate platform development in the Southern Iberian Palaeomargin (Prebetic of Alicante, SE Spain). BSGF - Earth Sci Bull 190:3. https://doi.org/10.1051/bsgf/2019001

Stein M, Arnaud-Vanneau A, Adatte T, Fleitmann D, Spangenberg JE, Föllmi KB (2012) Palaeoenvironmental and palaeoecological change on the northern Tethyan carbonate platform during the Late Barremian to earliest Aptian. Sedimentology 59:939–963

Vera JA (ed) (2004) Geología de España. SGE-IGME, Madrid

Vilas L (2001) El episodio extensional del Cretácico Inferior en el Prebético del altiplano de Jumilla - Yecla (Murcia). Geotemas 3:25–30

Vilas L, Arias C, Castro JM, Company M, García-Hernández M, de Gea GA, Ruiz-Ortiz PA (2004) Ciclo IV. In: Vera JA (ed) Geología de España. SGE-IGME, Madrid, pp 368–369

Weissert H, Lini A, Föllmi KB, Kuhn O (1998) Correlation of Early Cretaceous isotope stratigraphy and platform drowning events: a possible link? Palaeogeogr Palaeoclimatol Palaeoecol 137:189–203

Wissler L, Funk H, Weissert H (2003) Response of Early Cretaceous carbonate platforms to changes in atmospheric carbon dioxide levels. Palaeogeogr Palaeoclimatol Palaeoecol 200:187–205. https://doi.org/10.1016/S0031-0182(03)00450-4